

Impurity-induced states in unconventional superconductors: A promising technique to identify the pairing mechanism in HTS

Yanfei Yang

Department of Physics, Georgetown University, Washington, DC 20057

This paper reviews the properties of the theoretical predicted local virtual bound states induced by impurity in unconventional superconductors and the differential conductance data obtained in doped high temperature superconductor, BSCCO, using STM. The spatial patterns of the STM differential conductance resemble those of the impurity induced resonance states as predicted near the Fermi surface in many aspects, providing STM a promising method to understand the pairing mechanism in high temperature superconductors.

I. Introduction

To understand the fundamental rules behind the universal phenomena, scientists always prefer to study a pure system because impurities often cause great changes in the states of the system, making things much more complicated and detaining experimental testifying of the theories. However, in a later time, people found that controlled doping of impurities could achieve some desired properties. For example, the most salient application of impurities is in semiconductor industry. All transistors, building blocks of the semiconductor industry, consist of n-dope and p-doped semiconductors. In the solid-state laser industry, impurities are doped in the laser rod as the pumping source. More strikingly, not only used intentionally to achieve the desired properties of a system, impurities also help to understand properties of a pure system. This is the case in superconductors.

Impurity effects in superconductors were first noticed and studied in low temperature superconductors [1-5] in 1960s when people were still searching for higher temperature

superconductors. The pioneer work of Abrikosov and Gorkov [2] predicted the gapless superconductivity in the lowest Born approximation, which was observed by M. A. Woolf and F. Reif in 1965 [4]. This is followed by the realization that magnetic impurities may play the role of pairing breakers in s-wave superconductors. Further investigation [3] shows that magnetic impurity induced a bound state in the energy gap localized in the vicinity of the impurity atom, which grows to a bound states band and finally fills up the gap in the limit of finite impurity concentration. On the other hand, although the non-magnetic impurities will not change the bulk properties in conventional superconductors, they do have effects on the local density of states in a resonance scattering model [5].

Inspired by the prediction of the impurity effects on the local density of states, people realized that doping impurity provides a potential method to understanding the pairing mechanism in the unconventional superconductors, such as HTS, heavy fermion superconductors and other higher order superconductors. It has been predicted, also suggested by some experiment results [6-11], that high temperature superconductor has pairing states of $d_{x^2-y^2}$ symmetry. Both magnetic and non-magnetic impurities are pair-breakers in unconventional superconductors. Inner gap quasiparticle states induced by the nonmagnetic impurities will dramatically modify the local density of states around the impurities within a range of coherence length scale [12-15]. Measuring the tunneling current through the tip of a high resolution STM above the HTS surface, we can obtain the spectrum and spatial variation of the local density of states, which give information about the order parameter and pairing symmetry in high temperature superconductor [16-20].

The main purpose of this paper is to review the impurity effects on unconventional superconductors, especially high temperature superconductors, the current understanding of the impurity induced intragap states, and the latest experiment results. This paper is divided into four sections. In the second section, I will first introduce the BCS picture of quasiparticles in clean superconductors. In the third section, I will focus on the single impurity in d-wave superconductors. Then I will summarize in the last section.

II. BCS description of excited states in superconductor

A certain metal becomes superconducting below its transition temperature with the presence of Cooper pairs, which can transport in the metal with zero resistance. Cooper pair forms whenever there is an attractive interaction between electrons. In conventional superconductors, phonon-mediated scattering produces the attractive interactions between conductance electrons, resulting in the superconductivity and isotropic or nearly isotropic energy gaps for quasiparticles at the Fermi surface.

At zero temperature, the distribution of the probability of a Cooper pair, a couple of electrons with opposite wave vectors and spins ($\vec{k} \uparrow, -\vec{k} \downarrow$), being occupied resembles the normal metal Fermi function at T_c . At finite temperature below T_c , some Cooper pairs are broken and the electrons forming these Cooper pairs are excited to states that are not pairing for certain. There is a minimum excitation energy, Δ , for these excitation electrons so that the density of the excitation states is completely depleted.

According to BCS, the pairing Hamiltonian is

$$H = \sum_{k\sigma} \varepsilon_k n_{k\sigma} + \sum_{kl} V_{kl} c_{k\uparrow}^* c_{-k\downarrow}^* c_{-l\downarrow} c_{l\uparrow} . \quad (1)$$

Taking the zero of kinetic energy to be E_F , the Hamiltonian becomes

$$H = \sum_{k\sigma} \xi_k n_{k\sigma} + \sum_{kl} V_{kl} c_{k\uparrow}^* c_{-k\downarrow}^* c_{-l\downarrow} c_{l\uparrow} \quad (2)$$

where $\xi_k = \varepsilon_k - E_F$, V_{kl} are the matrix elements of the interaction potential, $n_{k\sigma}$ is number operator, $c_{k\sigma}^*$ and $c_{k\sigma}$ are the creation and annihilation operators, respectively.

Using canonical transformation and then diagonalizing the model Hamiltonian, we obtain

$$H = \sum_k (\xi_k - E_k + \Delta_k b_k^*) + \sum_k E_k (\gamma_{k0}^* \gamma_{k0} + \gamma_{k1}^* \gamma_{k1}) \quad (3)$$

where

$$c_{-k\downarrow} c_{k\uparrow} = b_k + (c_{-k\downarrow} c_{k\uparrow} - b_k) \quad (4)$$

$$\gamma_{k0}^* = u_k^* c_{k\uparrow}^* - v_k^* c_{-k\downarrow} \quad (5)$$

$$\gamma_{k1}^* = u_k^* c_{-k\downarrow}^* - v_k^* c_{k\uparrow} \quad (6)$$

$|v_k|^2$ is the probability for the pair $(\vec{k} \uparrow, -\vec{k} \downarrow)$ to be occupied and $|u_k|^2$ is the probability for the pair not being occupied. γ_{k0}^* (γ_{k1}^*) is the operator that creates an electron in $k \uparrow$ ($-k \downarrow$) state with a probability of 1. On the other hand, γ_{k0} (γ_{k1}) is the operator that annihilates an electron in $k \uparrow$ ($-k \downarrow$) state with a probability of 1.

The first term in Eq. (3) is BCS ground state energy term, while the second term represents the quasiparticle excitations of the system, which are often called *Bogoliubons*.

The energies of the excitation states are found to be

$$E_k = \left(\xi_k^2 + |\Delta_k|^2 \right)^{1/2} \quad (7)$$

In the BCS approximation that $V_{kl} = -V$, $\Delta_k = \Delta$ is a constant. Clearly, Δ_k is the minimum excitation energy for the *Bogoliubons*.

The density of the excitation states is

$$\frac{N_s(E)}{N(0)} = \begin{cases} \frac{E}{(E^2 - \Delta^2)^{1/2}} & (E > \Delta) \\ 0 & (E < \Delta) \end{cases} \quad (8)$$

Clearly, in a clean superconductor the density of states are depleted in the energy gap. All states are pushed above the energy gap, forming two peaks at the gap edge $\pm \Delta$.

III. Impurity problems in high temperature superconductors

All high temperature superconductors have strongly layered crystal structure containing one or more CuO_2 planes with copper and oxygen atoms in a square lattice, which is believed to be responsible for the superconductivity. Although the microscopic picture is still not clear, it is believed that the superconductivity in HTS is based on Cooper pairs of spin singlet form [22-29]. However, the pairing mechanism has not been confirmed and the microscopic theory for HTS is still lacking. Present knowledge of the superconductivity in HTS includes that electron interaction in HTS is pretty strong spin-fluctuation mediated interaction depending on both frequency and momentum [33], unlike the phonon-mediated weak interaction between Cooper pairs in conventional superconductors, and such an interaction favors $d_{x^2-y^2}$ pairing and gives rise to a momentum-dependent gap which has four nodes. The flux quantization experiments only support the d-wave pairing but can not give information about the specific pairing symmetry, for example, $d_{x^2-y^2}$ as proposed by N.E. Bickers et al. [30-37]. Measuring energy gap symmetry provides complementary evidence of the pairing mechanism. For example, angle-resolved photoemission spectroscopy (ARPES) can measure the gap energy along different directions in k space. As the prediction for $d_{x^2-y^2}$ pairing, a gaplike

feature is found to develop below T_c along the k_x and k_y direction, but not along the directions rotated by $\pi/4$ from them in the a-b plane.

Recently, more convincing evidences for $d_{x^2-y^2}$ pairing are found in experiments measuring the impurity induced quasiparticle states inside the energy gap in low temperature. The impurity induced quasiparticle states are usually localized in a microscopic or mesoscopic scale. Thus detecting of these states only become feasible after the development of high-resolution STM. The quasiparticle states are probed by measuring the differential conductance, which is proportional to the local density of states of the sample at the tip position. The experimental results [17-20] of the local density of states in BSCCO are strikingly consistent with theoretical prediction [12,14,38].

I will review some important results that support the $d_{x^2-y^2}$ pairing symmetry in HTS in the past decade. Impurity induced intragap states in unconventional and anisotropic superconductors have been extensively studied since 1993. The requirement and properties of the nonmagnetic impurity induced quasiparticle states in d-wave superconductors was discussed in detail by A.V. Balatsky *et al.* in 1995 [12]. I will basically following their calculation to give the spectrum and spatial variation of the quasiparticle states and compare some later experimental results with the predictions.

a) Single nonmagnetic impurity in d-wave superconductors

A single nonmagnetic impurity in unconventional superconductors is usually considered as a scattering scalar potential, $U = U_0 \delta(r - r_0)$, with the impurity at r_0 . The scattering of a quasiparticle from a single impurity in *d-wave* superconductor can be

described by a T matrix, $T(\omega)$, which is independent of wave vector. The Green function in the presence of a single impurity is

$$G_{\vec{k}\vec{k}'}(\omega) = G_{\vec{k}}^{(0)}(\omega)\delta_{\vec{k}\vec{k}'} + G_{\vec{k}}^{(0)}(\omega)T(\omega)G_{\vec{k}'}^{(0)}(\omega) \quad (13)$$

Where both $G_{\vec{k}}^{(0)}(\omega)$ and $T(\omega)$ are in Nambu space. The impurity induced states are given by the pole of the T matrix. Solving the poles of the T matrix for d-wave superconductor, we can find the energy of these states to be

$$\Omega = \Omega' + i\Omega'' = \Delta_o \frac{\pi c / 2}{\ln(8 / \pi c)} \left[1 + \frac{i\pi}{2} \frac{1}{\ln(8 / \pi c)} \right] = \Omega' + i\Omega'' \frac{\pi / 2}{\ln(8 / \pi c)} \quad (14)$$

where $c = \cos \delta_0$, indicating the strength of the scattering. δ_0 is the phase shift due to the impurity scattering. As c approaches 0, the system approaches unitary limit and the scattering gets stronger and stronger. For a weak scattering, $c \ll 1$. In the Born approximation limit, $c \gg 1$. Eq. (14) shows that the energy of the quasiparticle state is a complex value with the real and imaginary parts representing the energy and decay rate of the impurity induced state, respectively. So, these states are usually called virtual bound states due to the finite decay rate, in contrast to the bound states induced by magnetic impurities in conventional superconductors. In the unitary limit, $c \rightarrow 0$ and $\cos \delta \rightarrow \pi / 2$, the decay rate gets infinitely small and the virtual bound states becomes a marginally bound one at zero energy. In the weak scattering limit, the energy of the virtual bound state approaches Δ_0 . In the Born approximation limit, no bound state is found. (Fig 1)

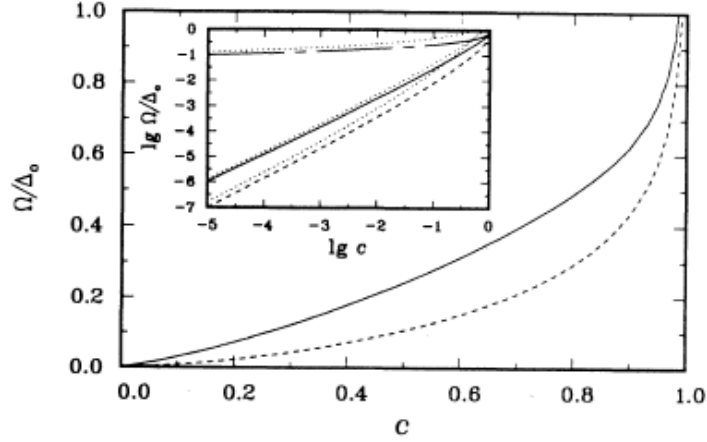


Fig. 1. the energy $\Omega = \Omega' + i\Omega''$ of the virtual bound state in the one-impurity problem, given by Eq. (x), as a function of impurity strength c : the shown quantities are Ω' (solid line), Ω'' (dashed line), and Ω''/Ω' (chain-dashed line). A spherical Fermi surface and $\Delta_{\vec{k}} = \Delta_0 \cos 2\varphi$ have been assumed. The width Ω'' of the virtual bound state is always smaller than its energy Ω' in the neighborhood of unitary scattering. In contrast, for weak scattering $c \sim 1$, $\Omega'' \sim \Omega'$ and an impurity-induced virtual state does not exist. The inset shows a comparison between the exact result and the asymptotic approximation (dotted lines), as computed to logarithmic accuracy by Eq. (x) for Ω [12]

Plots in **Fig 1** are the exact numerical results of the energy and decay rate of the single nonmagnetic impurity induced state as a function of c . **Fig 1 indicates** that a strong interaction potential is the requirement for the virtual bound states to exist in the energy gap. Thus, for a point scattering potential, $U = U_0 \delta(r - r_0)$, the density of the quasiparticle states localized around the impurity site will be greatly enhanced.

The enhanced local density of states in HTS was observed in $\text{Bi}_2\text{Sr}_2\text{CaCu}_2\text{O}_{8+\delta}$ (BSCCO) single crystals by Hudson et al. at low temperature [17]. In contrast to the expectation of a uniform differential conductance map at zero bias (voltage between tip and sample) in clean BSCCO samples, a large number of randomly distributed similar bright area with a diameter of about 3 nm were observed (**Fig 2a**). These atomic bright features are interpreted as the enhanced LDOS near the Fermi surface, referred as quasiparticle scattering resonances (QPRSs) in the original paper. The diameter of the bright area is consistent with the prediction of localization of the impurity induced quasiparticle

in the energy gap. The measurement of the differential conductance as a function of sample bias in a clean area (black area in Fig 2a) and a QPRSs area (Fig 2b) show very different features. The superconducting peaks, which indicate the quasiparticle states pushed to the edges of the energy gap, are suppressed at the center of a QPRS, implying the superconductivity being destroyed. The small lump in the middle of the energy gap peaking below the Fermi level indicates the quasiparticle states induced by scattering from an attractive potential. Both the low-energy LDOS feature and the diameter of the QPRSs are consistent with the prediction of Balaktsky et al. remarkably [14].

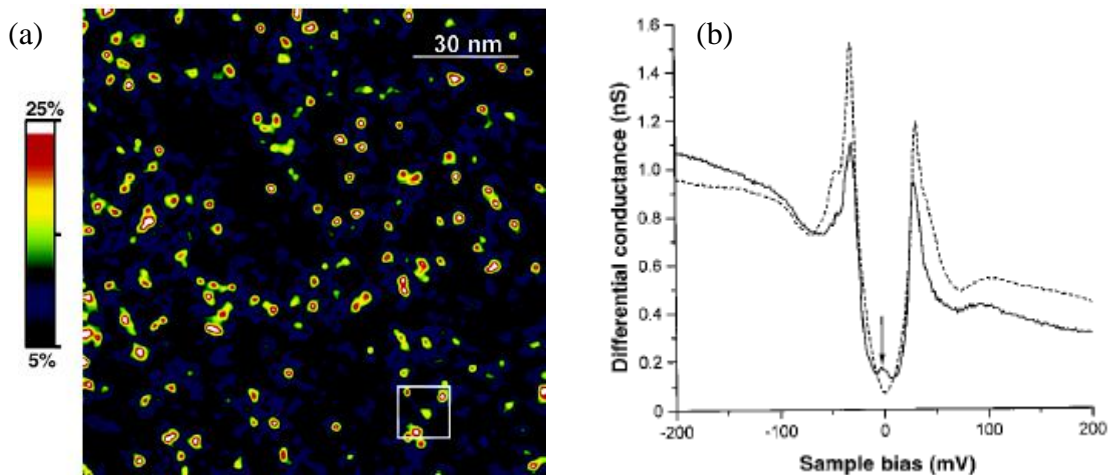


Fig 2. (a) A 130-nm square zero-bias conductance map in BSCCO single crystal. The color scale is in terms of percentage of normal state conductance. (b) Differential conductance versus bias voltage. The dashed line is taken in a clean area and the solid line is taken in a QPRS area. [17]

With the controlled doping of impurities, strong QPRSs were observed in Zn-doped and Ni-doped BSCCO (Fig 3a,b). In addition, vacancy induced quasiparticle states (Fig 3c) were proposed because of its universal existence in a large variety of samples, including impurity doped and undoped ones.

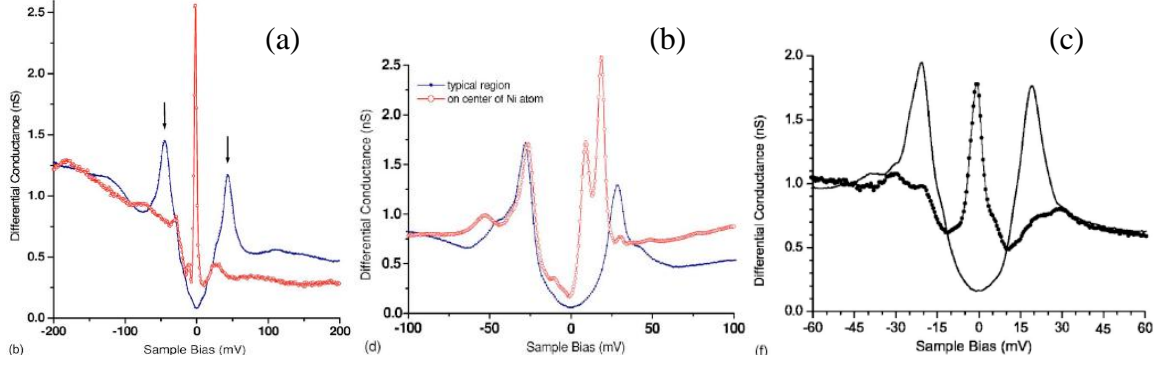


Fig 3. (a) Comparison of spectra directly above Zn impurity site (red) and the site far from impurity (blue) [19]; (b) comparison of spectra directly above Ni impurity site (red) and away from Ni (blue) [39]; (c) comparison of spectra directly above native defect (thick solid line) and away from defect (thin solid line) [20, 39];

b) Spectrum of the virtual bound states at the strong scattering impurity sites

As mentioned before, a strong scattering potential is the requirement to induce the quasiparticle states and then enhance the LDOS enough to be detected by STM. The strongly scattering impurity is pair-breaker in d-wave superconductors, producing dissimilar spectrum for hole-like and electron-like quasiparticles, and create distinct spatial variation features for the quasiparticle scattering resonances [14].

In the strong scattering case, the density of states is negligible at high energy $|\omega| \gg \Omega'$, and recovers the clean superconductor states at $|\omega| \ll \Omega'$, where ω is the probe energy of STM and Ω' is the resonance energy. So we will focus on the QPRSs spectrum for $|\omega| \sim \Omega'$ at the impurity site (Fig 4). The hole-like QPRS spectrum (Fig 4b) peaks around the resonant energy and obtain the maximum amplitude at $\omega = -\Omega'$. As ω decreases, the peaks get sharper but weaker and the virtual bound state reduces to a marginally bound state at zero energy. As ω increases, the peak persists to $c \sim 1$, where it disappears as a broad structure. On the other hand, the electron-like QPRS spectrum (Fig 4b) only shows

a shallow feature in this regime. This feature dominates while $r \ll l_F$, where $l_F = 2\pi/k_F$ is the Fermi length.

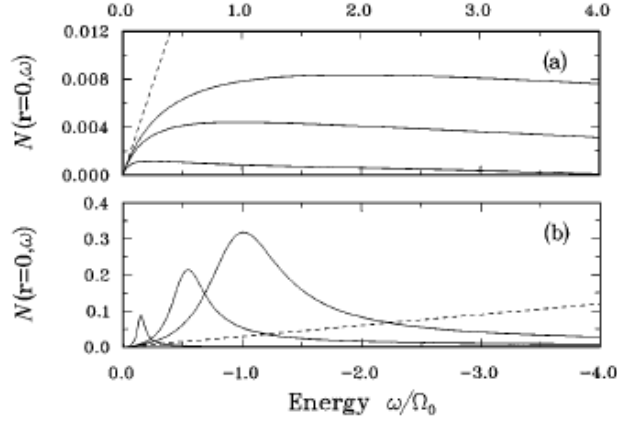


Fig 4 The local density of states $N(r=0, \omega)$ of a d-wave superconductor for (a) $\omega > 0$ and (b) $\omega < 0$ at the impurity site as a function of energy ω for $c = 0.02, 0.06,$ and 0.10 (from bottom to top). Here, $\Omega_0 = 0.03 \Delta_0$ is the impurity resonance energy for $c = 0.10$. The density of states $N_0(\omega) = |\omega|/\Delta_0$ of a clean d-wave superconductor is shown by the dashed line. Note the different density scales.

c) Spatial variation of the quasiparticle resonance states

The QPRS states are localized [40, 14] to the impurities in a scale comparable to the coherence length of the superconductor. In d-wave superconductors, the density of the impurity states, $N_{imp}(\vec{r}, \omega)$ decays as the inverse second power of r , the distance from the impurity, along the nodes of the gap function,

$$N_{imp}(\vec{r}, \omega = 0) \propto \text{Re}[G^{(0)}(\vec{r}, \omega = 0)]^2 \propto r^{-2} \quad (15)$$

and exponentially in the vicinity of the extrema of the gap function,

$$N_{imp}(\vec{r}, \omega = 0) \propto [\xi(\varphi)/r] e^{-2r/\xi(\varphi)} \quad (16)$$

where $\xi(\varphi) = \hbar v_F / |\Delta(\varphi)|$ is the angle-dependent coherence length of the superconductor.

$N_{imp}(\vec{r}, \omega)$ gets saturated at $r > l_0$, where $l_0 = \hbar v_F / \Omega'$ is the impurity induced length [12].

More detailed and rapid varying features [14] of $N_{imp}(\vec{r}, \omega)$ occur at a distance comparable to three characteristic lengths: $l_F = 2\pi/k_F$ is the Fermi length, $\xi_0 = \hbar v_F / \Delta_0$ is the coherence length of the superconductor and l_0 , the impurity induced length. The requirement of these characteristic lengths for the virtual bound state is $l_F \ll \xi_0 \ll l_0$.

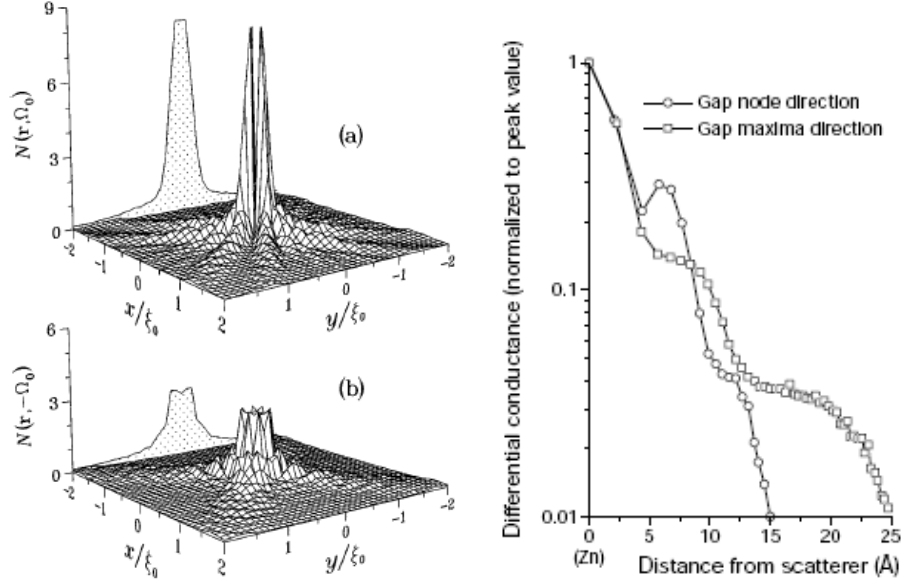


Fig 5 The local density of states $N(\vec{r}, \omega)$ of a d-wave superconductor for (a) $\omega = \Omega_0$ and (b) $\omega = -\Omega_0$ as a function of position $\vec{r} = (x, y)$ around a repulsive impurity placed at $\vec{r} = 0$. The impurity resonance energy is $\Omega_0 = 0.0.3 \Delta_0$ and $\xi_0 / l_F = 6$. The maximum values of $N(\vec{r}, \pm\Omega_0)$ are approximately 8.3 and 2.9 (in units of N_F). The shaded profile shows the projection of $N(\vec{r}, \pm\Omega_0)$ on the vertical plane. [14] (c) differential tunneling conductance at resonance energy versus distance r from the center of a Zn scatterer, along the a-axis or b-axis (gap-node) directions (shown as open circles) and along the Cu-O bond (gap-maxima) directions (shown as open squares). Each data point is the local DOS at distance r averaged over an inclusive angle of 10° around the given directions [19]

Fig 5a, 5b show the calculation of the spatial variation of the local density of states of a d-wave superconductor when the STM bias voltage set at resonance energy Ω' . At distances $r \ll \xi_0$, the density of the states is most strongly enhanced in the horizontal and vertical directions (the extrema directions of the d-wave energy gap) for both hole-

like and electron-like states. As the distances increase to $r \sim \xi_0$, the density of states is enhanced along the diagonal directions for the hole-like resonance ($\omega = -\Omega'$) and in the directions close to the diagonals for the electron-like resonance ($\omega = \Omega'$). Further away, the density of states decays quickly to be saturated. Fig 5c shows the spatial variation of the differential conductance (normalized to peak value) around an impurity in Zn-doped BSCCO along both the gap-node and gap-maximum directions. Although these data can not be fit to the power law and exponential law as predicted in Eq. (15) and Ea. (16), the decay rate is clearly faster in the gap-node directions.

These predicted star-like patterns of the density of QPRSs have been observed in Zn-doped and Ni-doped BSCCO samples (Fig 6).

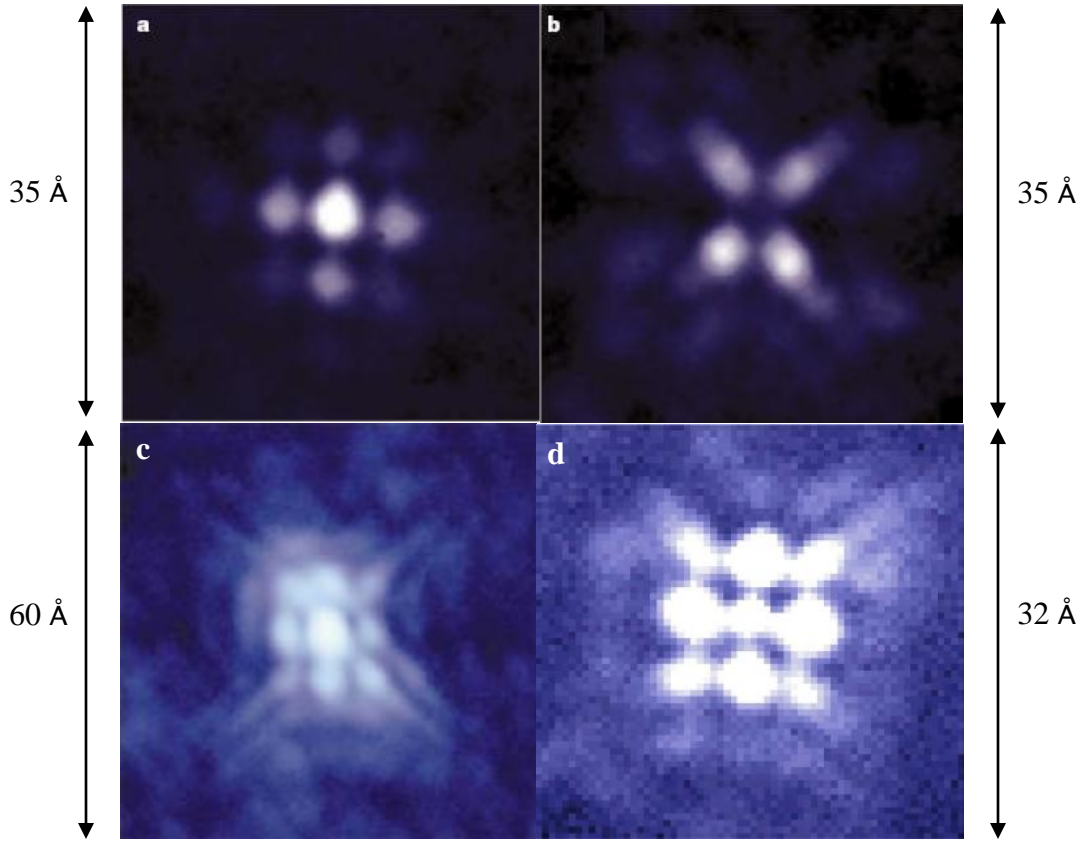


Fig. 6. Experimental STM impurity spatial patterns at resonance [39] (a) STM intensity around Ni impurity site at 9 mV [18]; (b) STM intensity around Ni impurity site at -9 mV [18]; (c) STM intensity around Zn impurity site at -1.2 mV [19]; (d) STM intensity around native defect, possibly Cu vacancy at -0.5 mV [20]

Even with the striking observation of the four fold local QPRSs pattern around the impurity in BSCCO that is consistent with many models, discrepancies exist between the predicted local DOS and the measured data by STM. All the experiment data were obtained on the non-superconducting BiO crystal layer and thus it is not sure that the intrinsic wave function in the superconducting CuO layer is measured. On the other hand, an accurate calculation of the wave function of the impurity induced bound states in the energy gap is still lacking. The impurity scattering potentials in the previous models were all simplified as pointlike scalar potentials, which may also contribute to the discrepancies. Recent ab initio calculation of the impurity in CuO layer [39] shows that the effective magnitude of the potential of three kinds of impurity (Zn, Ni, and vacancy in and on CuO plane) is consistent with phenomenological fits of previous scalar potential models to STM resonance energies, but the effective potential ranges are quite short of order 1 Å with weak long-range tails. More strikingly, all the potentials are remarkably anisotropic in space, oscillating between repulsive and attractive potentials from the impurity center.

IV. Summary

In this paper, I reviewed the simplest model of the single nonmagnetic impurity problem in HTS and corresponding STM data. These models predicted the intragap virtual bound state induced by nonmagnetic impurity, which can modulate the local density of states around the impurity dramatically. These virtual bound states are localized to the impurity in a scale comparable to the coherence length in the superconductor. The density of QPRS states enhanced dramatically around the impurity in a scale of coherence length along both the gap-node and gap-maximum directions in

the d-wave superconductors while the decay rates of the resonance state wave function obey a power law along the gap-node direction and an exponential law along the gap-maximum direction, resulting in an oscillating star-like pattern of the local density of states. STM is proposed as a singular tool to detect the spatial pattern of the QPRSs due to its particular sensitivity to the DOS near Fermi energy and its ability to measure both the local density of states and the topography of superconductors in atomic scale at the same time. The pairing mechanism and the gap symmetry then can be deduced from the differential conductance obtained by STM above the impurity sites. However, detail form of the impurity scattering potential and long-range hopping between impurities should be considered and may give a better explanation of the discrepancy between the theoretical prediction and the real LDOS pattern obtained by STM. A more detail and complete review about the impurity induced bound states in unconventional superconductors has been done by Balatsky *et al.* [41]

Reference:

- ¹P.W. Anderson, *Phys. Rev. Lett.* 3, 325 (1959)
- ²A. Abrikosov and L.P.Gor'kov, *Soviet Phys. JETP* 12, 1243 (1961)
- ³L. Yu (1965); H. Shiba (1968)
- ⁴M. A. Woolf and F. Reif, *Phys. Rev.* 137, A557 (1965)
- ⁵K. Machida and F. Shibata, *Prog. Theor. Phys.* 47, 1817 (1972)
- ⁶D. R. Harshman *et al.*, *Phys. Rev. B* 39, 851, (1989)
- ⁷S.E. Barrett, *Phys. Rev. Lett.* 66, 108 (1991)
- ⁸M. Takigawa, J. L. Smith and W. L. Hults, *Phys. Rev. B* 44, 7764 (1991)
- ⁹L. Krusin-Elbaum *et al.*, *Phys. Rev. Lett.* 62, 217 (1992)
- ¹⁰T. R. Thurston *et al.*, *Phys. Rev. B* 46, 9128 (1992)
- ¹¹Z-X. Shen *et al.*, *Phys. Rev. Lett.* 70, 1553 (1993)
- ¹²A.V. Balatsky, M.I. Salkola and A. Rosengren, *Phys. Rev. B* 51, 15547 (1995)
- ¹³C.H. Choi, *Phys. Rev. B* 50, 50 (1994)
- ¹⁴M.I. Salkola, A.V. Balatsky and D.J. Scalapino, *Phys. Rev. Lett.* 77, 1841 (1996)
- ¹⁵A.P. Kampf, *Phys. Rev. B* 56, 2360 (1997)
- ¹⁶A. Yazdani *et al.*, *Phys. Rev. Lett.* 83, 176 (1999)
- ¹⁷E.W. Hudson *et al.*, *Science* 285, 88 (1999)
- ¹⁸E.W. Hudson *et al.*, *Nature* 411, 920 (2001)
- ¹⁹S.H. Pan *et al.*, *Nature* 403, 746 (2000)
- ²⁰E.W. Hudson *et al.*, *Physica B* 329, 1365 (2003)
- ²¹Shiba, *Prog. Theor. Phys.* 50, 50

- ²²D. Esteve *et al.*, *Europhys. Lett.* 3, 1237 (1987)
- ²³E. Gough *et al.*, *Nature* 326, 855 (1987)
- ²⁴R. H. Koch *et al.*, *Appl. Phys. Lett.* 51, 200 (1987)
- ²⁵P. L. Gammel *et al.*, *Phys. Rev. Lett.* 59, 2592 (1987)
- ²⁶H. F. C. Hoevers, *Physica C* 152, 105 (1988)
- ²⁷S. E. Barrett, *Phys. Rev. Lett.* 66, 108 (1991)
- ²⁸S. E. Barrett, *Phys. Rev. B* 41, 6283 (1990)
- ²⁹M. Takigawa, *Phys. Rev. B* 39, 7371 (1989)
- ³⁰D. J. Scalapino *et al.*, *Phys. Rev. B* 34, 8190 (1986)
- ³¹K. Miyake *et al.*, *Phys. Rev. B* 34, 6554 (1986)
- ³²N. E. Bickers *et al.*, *Phys. Rev. Lett.* 62, 961 (1989)
- ³³P. Monthoux and D. Pines *Phys. Rev. Lett.* 69, 961 (1992)
- ³⁴P. Monthoux, A. V. Balatsky, and D. Pines, *Phys. Rev. Lett.* 67, 3448 (1991)
- ³⁵P. Monthoux, A. V. Balatsky and D. Pines, *Phys. Rev. B* 46, 14803 (1992)
- ³⁶P. Monthoux, D. Pines, *Phys. Rev. B* 49, 4261 (1994)
- ³⁷P. Monthoux, D. J. Scalapino, *Phys. Rev. Lett.* 72, 1874 (1994)
- ³⁸J.M. Byers *et al.*, *Phys. Rev. Lett.* 71, 3363 (1993)
- ³⁹L.-L. Wang, P. J. Hirschfeld, and H.-P. Cheng, *Phys. Rev. B* 72, 224516 (2005)
- ⁴⁰Patrick A. Lee, *Phys. Rev. Lett.* 71, 1887 (1993)
- ⁴¹A.V. Balatsky, L. Vekhter and Jian-Xin Zhu, arXiv: cond-mat/0411318 (2004)